DOI: 10.61782/fa.2023.1282

forum acusticum 2023

Drone and eVTOL flyover noise simulation - comprehensive process from aeroacoustics to sound quality

Patrick Boussard[1*] **Domenico Caridi**[2] **Alexandre Bouthéon**[3]
Antoine Minard[3] **Shouvik Bandopadhyay**[3]
[1] Ansys, Technopole de l'Arbois, 13100 Aix-En-Provence, France
[2] Ansys, Via G. B. Pergolesi 25, 20124 Milano, Italy
[3] Ansys, 35-37 Rue Louis Guérin, 69100 Villeurbanne, France

ABSTRACT

Drones and eVTOLs will definitely be a part of the city of tomorrow. How big a part they will play strongly depends on community noise management and acceptance from city populations. This paper proposes a comprehensive process to simulate, study and reduce the annoyance of such noise sources. A large part of the noise is coming from the rotor blades and can be simulated with aeroacoustics computation tools, which also account for the interferences produced between several rotors. Other sources such as the e-motor also play an important role that needs to be considered. The impact of the propagation of these source noises towards the ground is quite different at small and large distances, and different modeling approaches can be used (source directivities, atmospheric absorption, turbulence, etc.). Then, various techniques can be employed for the spatial sound rendering of the noise perceived on the ground; this paper considers two approaches: binaural rendering over headphones and Vector-Base Amplitude Panning with a multiple-speaker system. Finally, psychoacoustics indicators can be calculated on the simulated noise and then compared to listening test results.

Keywords: *eVTOL, drone, Aerocoustics, flyover noise, annoyance.*

1. INTRODUCTION

Recent years have seen a large increase of multi-rotor drone usage, as application fields multiplied: recreational remote piloting, marketing videos, security, civil engineering, etc. But this drone usage often remains far from inhabited areas, and the study the associated noise pollution was generally not a major concern. However, new urban purposes are rising as possible use cases in the near future that can only affect these areas, such as drone delivery for example. As populated areas will most definitely be more affected by these drone use cases, the question of the emitted noise has received much more interest.

The near future should see another type of multi-rotor vehicle to transport passengers over short urban distances. Although this new means of transportation has not been really put in use yet, concerns have already been raised about the associated noise pollution. Anticipating the noise impact, as well as finding mitigating solution, is thus quite difficult as there is only limited experimental data available on a large scale on which to base noise impact research. It is thus paramount to find efficient modelling tools for the prediction of the noise of such sources perceived at the ground. Thankfully, the acoustics of these vehicles share a lot with unmanned drones, which provide much more experimental data. Multi-rotor vehicles, whether manned or unmanned, are generally commonly referred to as VTOL (Vertical Take-Off and Landing), or eVTOL when an electrical power source is used.

VTOL aircraft market is emerging for Advanced- and Urban Air Mobility (AAM, UAM) as a potential transportation solution to bypass the urban roadway traffic, where other aerial rotorcraft are unfit for operation due to their excessive noise. NASA Emerging Aviation Markets Tiger Team proposed a classification of these new markets into 4 categories depending on propulsion type, number of passengers (if any), and typical flight altitude, speed, and range [1]:

- Remote Controlled Unmanned Drone (including typical recreational drones)
- Urban Air Mobility
- Short Haul Aircraft

[*] ***Corresponding author***: patrick.boussard@ansys.com.

- Unmanned Aircraft Systems/High Altitude Long Endurance

However, as the production and operation of these aircraft increase, especially at relatively low altitudes in proximity of highly dense civilian areas, their noise becomes the cause of annoyance. Prolonged exposure to such noise may also lead to hearing/nervous system ailments in the longer term [2].

In an effort to mitigate the harmful effects of the noise from eVTOLs, regulatory agencies like FAA and EASA have imposed several restrictions on the manufacturers regarding the acoustic emission footprint of their products. Any new products need to be certified for airworthiness before entry to market in accordance with these norms [3,4,5].

Therefore, releasing new products into the market requires their manufacturers to perform 2 central tasks related to acoustics: (i) Reduce the noise emitted from their products (drones/eVTOLs) and (ii) Quantify the acoustic footprint and the perceived noise levels by observers for the certification process.

Much like it was done in the past for commercial aircraft [6], this paper describes how the modelling of the acoustic phenomena put into play during a VTOL flyover, broadly summarized in Fig. 1, can help predict the noise that will be perceived at the ground. This is applied to the case of a small commercial drone and a mid-size professional drone (although only partly presented here).

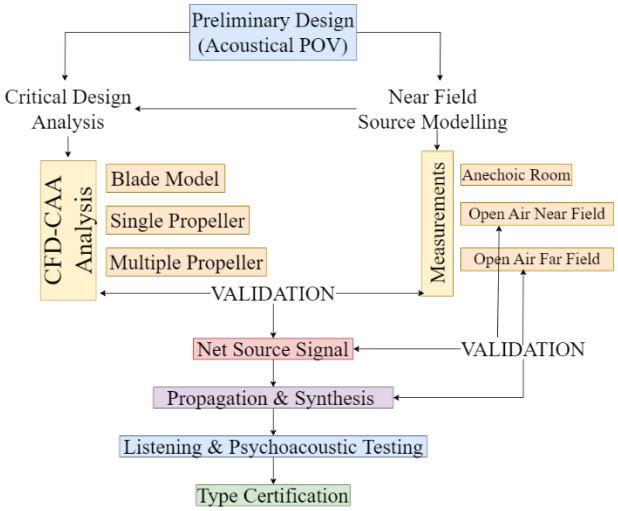

Figure 1. Drone/eVTOL Product Development Cycle from the acoustics point of view.

2. AEROACOUSTIC SIMULATION OF SOURCES

Computational Aeroacoustics refers to the simulation and prediction of the noise generated by the interaction of moving air with solid surfaces and self-generated noise due to turbulence. When a propeller is considered, this interaction can generate different kinds of noise sources: steady and unsteady ones [7].

Steady sources involve linear thickness, linear loading, and (nonlinear) quadrupole. At moderate low speed, when the tip is far from transonic condition, non-linear effects can be neglected, and the linear thickness and loading dominate. Unsteady sources are time-dependent in the rotating-blade frame of reference. They include periodic and random variation of loading on the blades. A typical example of periodic blade loading in propellers is the effect of shaft angle of attack which is typical of drones in all flight conditions where they do not simply hover vertically and negligible wind is present. All non-uniform inflow conditions contribute to unsteady loading, including blade and fuselage vortex generation and interactions with other blades. Unsteady random sources give rise to broadband noise. This can happen in case the inflow is turbulent and hits the leading edge of the blade and also as a result of the turbulent boundary layer development on the blade itself. When the turbulent boundary layer reaches the trailing edge, it generates broadband noise as well as when the tip vortex shedding interacts with the blade tip and trailing edge surfaces.

In the frame of Computational Fluid Dynamics (CFD) many numerical methods are suitable to compute and propagate the noise generated from drones and eVTOLs rotors and its fuselage, we briefly mention:

- CAA, Computational Aero Acoustics.
  It involves the computation of the noise source and propagation by highly accurate CFD compressible simulations.
- Wave Solver Methods and Acoustic Analogy. They both decouple the noise source computation from the propagation under certain assumptions, e.g. the acoustic feedback on the flow is negligible. The noise sources are computed by an accurate CFD simulation for both methods, the difference is in how the propagation is accounted for. In the Wave Solver Methods, the noise propagation is indeed computed using wave solver methods which are available in many flavors. On the other hand, the Acoustic Analogy such as Ffowcs Williams and Hawkings (FW-H) relies on integral methods and compute the noise propagation with an analytical formulation

generally based on the free space Green's function, thus assuming no obstacles between the source and the receiver. This method is very computationally efficient and reliable.

Ansys Fluent implements all the above methods to accurately and efficiently predict the noise generated from the rotors and fuselage of drones, eVTOL and other aircraft configurations.

One relevant aspect of the CFD simulation is that it does not only produce time pressure signals results at prescribed microphone locations but gives insight into where the noise sources originate and their strength. It is also possible to perform detailed post-processing analysis to extract more information which is key to the designer to improve the acoustics quality performance. This is generally very difficult or impossible to achieve through physical testing, e.g. getting the dipole noise source distribution in frequency domain, helping to understand the connection between flow dynamics and noise generation mechanism (example in Fig. 2), visualizing the noise propagation pattern, highlighting critical design areas, etc.

Figure 2. CFD simulation and visualization of the complex unsteady turbulent structures generated by the rotors of a quadcopter, using Ansys Fluent.

3. MODELING PROPAGATION TO THE GROUND

Controlled acoustic measurements allow capturing near-field, spectral or time-domain data, at different angular positions around each propeller. Alternatively, these data can be produced by simulation, as detailed in section 2. In either case, the noise perceived at the listening position on the ground is strongly different, as these sources' emitted noises are affected by various propagation phenomena on the way.

In the context of drone noise, the propagation mechanism is strongly dependent on a variety of propagation and operational factors. Fig. 3 and Fig. 4 illustrate a couple of such phenomena, wherein, data was obtained through an open-air experimental campaign of a DJI Quadcopter, with the repeatability index 0th order.

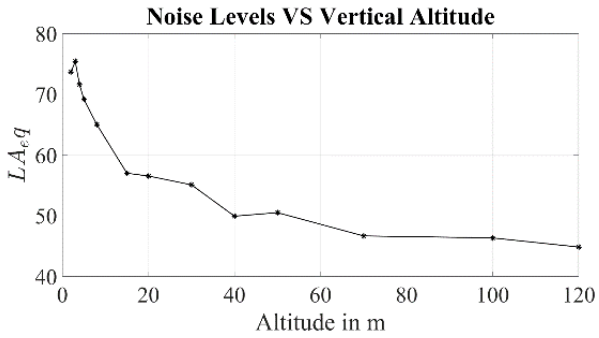

Figure 3. Effect of vertical distance attenuation on the sound level.

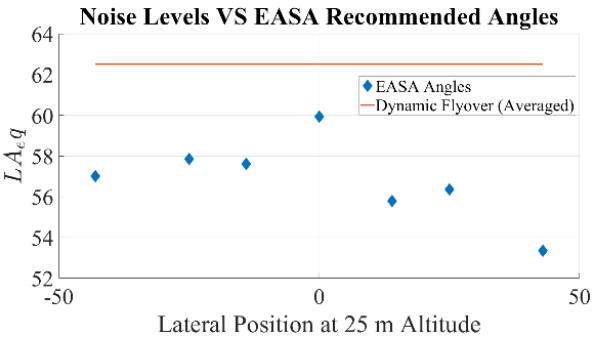

Figure 4. Drone noise - Static hovering vs. Dynamic flyover.

Fig. 3 illustrates an inverse relationship of the sound level with respect to the distance between the source and the listener. Fig. 4, however, illustrates that more variables come into play apart from just the distance. For instance, the scatter plot shows that the sound level is not the same at different positions with the same source/receiver distance (here laterally opposite). Moreover, the noise level emitted during dynamic flyover is higher than that of the noise emitted during static hovering across different lateral locations. A robust model of propagation, based on the physics of the interactions of various propagation factors

involved in the noise propagation, is needed to accurately capture these features. Experimentation helps in validation and hence, improvements of the models. The various phenomena that are to be accounted for are elaborated upon in subsections 3.1 through 3.5.

3.1 Geometrical spreading

Geometrical spreading, also known as distance attenuation, is a phenomenon in acoustic propagation where the intensity of sound waves decreases as they travel away from their source due to the spreading of the wavefront over a larger area.

Before calculating the geometrical spreading, it is important to define the type of acoustic source. As a first simple approach, each propeller can be assumed to be a point source, wherein, the Geometric spreading A_geo (t) in dB may be quantified as:

$$A_{geo}(t) = 20\log_{10}\frac{1}{d(t)} \quad (1)$$

where $d(t)$ is the source-receiver distance in m.

A more realistic approach relies on a dipole source model to allow for better accuracy for both near-field and far-field acoustic propagation modeling. The main reason for that is the fact that each propeller in a drone/eVTOL produces sound by creating alternating areas of high and low pressure as the blades rotate. This effect is best represented by a dipole source, which has two equal and opposite point sources separated by a small distance. The dipole model captures the directionality of the sound emission and the spatial distribution of the pressure fluctuations more accurately than a single point source [8,9].

But computational implementation of n dipoles is complicated. A simplification that would reduce the computational complexity and account for the dipolar nature of the noise sources, is to model the n dipoles as one single equivalent dipole that accounts for each dipole individually as well as their mutual interactions [10,11].

The method to calculate the noise received in the far field at the listener's location while accounting for the Geometrical spreading using the equivalent dipole method is elaborated below:

The sound pressure level (SPL) at any point in the far-field can be calculated using the equation below:

$$SPL(t) = 20\log_{10}\left(\frac{p(t)}{p_0}\right) \quad (2)$$

Where,

$$p(t) = \frac{k}{4\pi d}\left|p_s(t)\cdot\widehat{s(t)}\right| \quad (3)$$

And,

$$k = \frac{2\pi f d}{Z} \;\; and \;\; Z = \rho c \quad (4)$$

In the above equations, k represents the factor of geometrical spreading, and Z represents the acoustic impedance of the medium of propagation. For a dipole source of equivalent dipole moment p_s and its equivalent location defined by the unit vector $\hat{s}$, the SPL at a point in the far-field can be expressed as:

$$SPL(t) = 20\log_{10}\left(\frac{f\left|p_s(t)\cdot\widehat{s(t)}\right|}{2\rho c p_0}\right) \quad (5)$$

3.2 Doppler Effect

The relative motion between the acoustic source and the listener causes a frequency ratio r_{dop} between the source and the listener position. This phenomenon is known as Doppler effect. This effect also produces a gain in dB A_{dop} between the source and listener. Both r_{dop} and A_{dop} depend on time, but are independent of frequency:

$$r_{dop}(t) = \frac{1}{1 - M(t)\cos\left(\beta(t)\right)} \quad (6)$$

$$A_{dop}(t) = 20\log_{10}\frac{1}{\left(1 - M(t)\cos\left(\beta(t)\right)\right)^2} \quad (7)$$

$M(t)$ represents the Mach Number as observed at the propeller tip. M is calculated according to the speed of the blade at the tip $V_{prop-tip}$, and on altitude h through the speed of sound c:

$$M(t) = \frac{V_{prop-tip}(t)}{c(t)} \quad (8)$$

where $c(t) = \sqrt{\gamma R(T_0 + ah(t))}$

In the above equations, $\gamma = 1.4$ (ratio of specific heats), $R = 287\ J.kg^{-1}K^{-1}$ (universal gas constant for air), $a = -0.0065\ K.m^{-1}$ (lapse rate), and $T_0 = 288.15\ K$ (temperature at the mean sea level).

3.3 Atmospheric attenuation

Atmospheric attenuation of sound is a combination of two factors: atmospheric absorption and atmospheric scattering, which both depend on time and frequency. The attenuation due to atmospheric absorption A_{abs} is given by the following formula [12]:

$$A_{abs}(t,f) = 10\,\alpha(t,f).d(t) \quad (9)$$

The attenuation due to atmospheric scattering A_{sca} is given by the following formula [12]:

$$A_{sca}(t,\lambda) = \frac{C_{sca}(t,\lambda).\lambda^2}{4\pi}\left(\frac{1}{d(t)^2}\right) \quad (10)$$

In the equations 9 and 10, d represents the distance between the source and the listener and $\lambda = \frac{c}{f}$ represents the acoustic wavelength. α and C_{sca} represent the absorption coefficient and the scattering coefficient respectively. The calculation of these coefficients may be done with the help of numerous existing empirical and semi-empirical models, depending on their applicability [13-16].

3.4 Ground reflection

If we suppose a specular reflection on the ground (flat surface, no diffusion, see Fig. 5), the noise received at the listening position corresponding to the sum of 2 waves: the direct wave from the source to the listening position, and the wave reflected on the ground. The reflected wave is affected differently as it propagates: different directivity value at the emission, longer path distance, and absorption by the ground.

In particular, the fact that the reflected path is longer not only modifies the calculated propagation parameters (different geometrical spreading, atmospheric attenuation, Doppler effect), but also means that the reflected wave arrives later. This delay will vary over time, depending on trajectory, and translates into a comb filtering in the frequency domain, whose pattern varies over time.

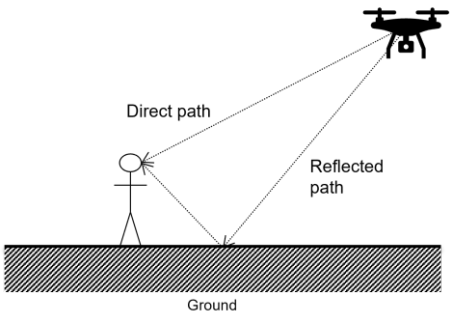

Figure 5. Ground reflection.

If we cannot suppose a specular reflection, then it is also important to consider the effect of incidence and reflection angles to satisfy cases of ground surfaces with varying topographies. A good approach to account for the ground interaction attenuation is given by Equation 11, which is obtained from the classical Ray Tracing method [17]. The technique involves modeling the wave or particle as many very narrow beams (rays) and advancing them through the medium by discrete amounts, considering the medium's properties and any reflecting surfaces.

$$A_{gr} = 10log_{10}\left(\frac{1-\eta^2}{1+\eta^2-2\eta cos(\beta_i)e^{-\alpha_g d_r}}\right) \quad (11)$$

In the above equation, α_g represents the absorption coefficient of the ground, which is dependent on the type of ground/reflecting surface. The η, β_i, and d_r represent the reflection coefficient, the incidence angle, and the distance of the reflected ray respectively. The equation 11 may be applied to n number of interacting/reflecting surfaces to account for the net interaction effect due to all the surface in a particular topographic region.

3.5 Atmospheric turbulence

Continuous/Discrete wind turbulence and/or Clear Air Turbulence (CAT) contribute to some part of the attenuation of the acoustic wave. It also contributes significantly to the modulation depth. Compared to empirical, semi-empirical and phenomenological models, Dryden's model [18] based on the (Homogenous Isotropic Turbulence) HIT [19] assumption offers 3 main advantages: (i) Ease of computational implementation, (ii) Better Consistency of statistical parameters, and (iii) Better Control over the randomness parameter.

The attenuation and the modulation depth due to atmospheric turbulence may be calculated with the equation 12 and 13 respectively.

$$A_T(t) = 10^{-4} f_c^{2/3} \int_0^{\infty} S_n(f) e^{-2\pi i f d(t)/z} df \quad (12)$$

$$M_T = \frac{\sqrt{\int_0^{\infty} S_n(f) df}}{f_c^{2/3}} \quad (13)$$

In the above equations, $S_n(f)$ represents the spectral density of turbulence which is quantified as:

$$S_n(f) = 4\overline{\sigma_v^2}\frac{f_c^2}{(1+f/f_c)^{5/3}} \quad (14)$$

Where σ_v is the standard deviation of the velocity fluctuations.

The Dryden model generates turbulence that is pseudo-random while still maintaining certain statistical properties that are consistent with real-world turbulence. In practice, the Dryden model can be implemented in a continuous or discrete form using band-limited white noise with appropriate filters or finite difference equations. The model's parameters, such as turbulence scale length and turbulence intensity, can be adjusted to match the desired frequency ranges and altitude-dependent properties. The

generated turbulence can be used as wind disturbance inputs for drones or other dynamic systems. The total attenuation of the acoustic wave before reaching the ground may now be computed as

$$A = A_{abs} + A_{geo} + A_T \quad (15)$$

and the total modulation may be calculated as

$$M = M_0 M_T \quad (16)$$

and

$$M_0 = \frac{1}{2} e^{-A/20} \quad (17)$$

4. 3D SOUND RENDERING

4.1 Audio synthesis of propagated acoustic data

Actual sound synthesis consists in transforming the spectro-temporal data at the receiving point into a sound pressure signal in the time domain. The broadband noise component is synthesized by the Overlap Add method [20]. This analysis-synthesis method is based on the decomposition of the time signal into a collection of successive overlapping windows. The algorithm creates a short-term spectrum in each window, which is then transformed into a time-domain signal through Inverse Fourier Transform and added to the overall signal. For each tonal component, an independent sinusoidal signal is created by means of a lookup table. The different generated signals are added together, and the ground reflection effect is eventually applied by adding the calculated signal for the reflected path.

4.2 3D flyover noise rendering

For realistic sound rendering purposes, the perception of the movement of the aircraft (front-rear trajectory and passing overhead) must be reproduced and the aircraft position at each instant must be the same at any angular position of the listener's head. For this reason, the spatial aspect of the aircraft flyover is rendered by using one of two available systems: through loudspeakers in an immersive room or through headphones.

In case of loudspeaker playback, a series of loudspeakers can be positioned on a semi-circle over the predefined listening position, and the sound playback is smoothly shifted from one loudspeaker to the other (Vector-Based Amplitude Panning technique) along the flyover duration.

In case of playback over headphones, the synthesized monophonic sound is transformed into a binaural sound in order to recreate the perception of a front-overhead-rear trajectory. This is carried out using HRTF filters (including interaural time and level differences – ITD and ILD – as well as spectral resonances created by reflection of the sound waves on the torso, shoulders, head and pinnae). These filters are adapted in real time according to both the virtual instantaneous position of the aircraft and the listener's head movement. The listener's head instantaneous position is determined using a headtracking sensor placed over the headband of the headphones. In this manner the virtual absolute position of the aircraft at any instant is maintained when the listener turns his head for example. This process is summarized on Fig. 6.

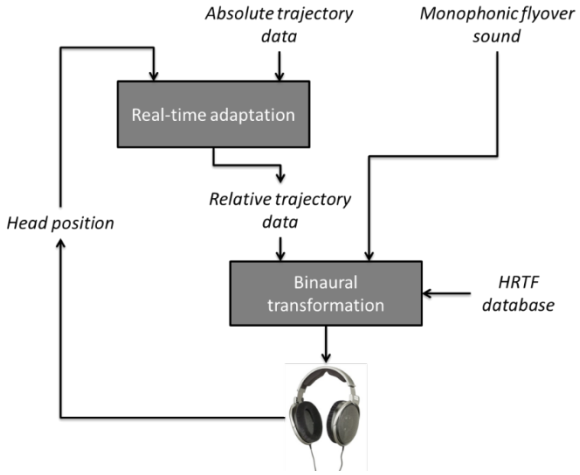

Figure 6. Diagram of the binaural transformation of the synthesized sound.

5. LISTENING TESTS AND PSYCHOACOUSTIC INDICATORS

The perceptual study of vehicle flyovers often relies on the conduction of listening tests in a controlled environment. The literature offers many examples of such studies, many of which deal with the case of commercial aircraft flyovers [21,22]. Depending on the question of interest, different listening test procedures can be used. Quite often, flyover-related annoyance is of the essence. In that case, test participants are asked to rate the unpleasantness of different flyover recordings or syntheses following a specific design of experiment.

Here, a such listening test was conducted on the syntheses obtained for a small commercial drone, and a mid-size professional drone. The listening test was conducted with Ansys Sound – Jury Listening Test. This tool makes it possible to very rapidly set up instructions and test interfaces for a listening test, in a very rigorous

psychoacoustic framework, and allow a first round of simple statistical analysis (average ratings, 95% confidence intervals, post-hoc tests for multiple comparisons). An example of such test interface is shown on Fig. 7. The actual results of the test are still under analysis.

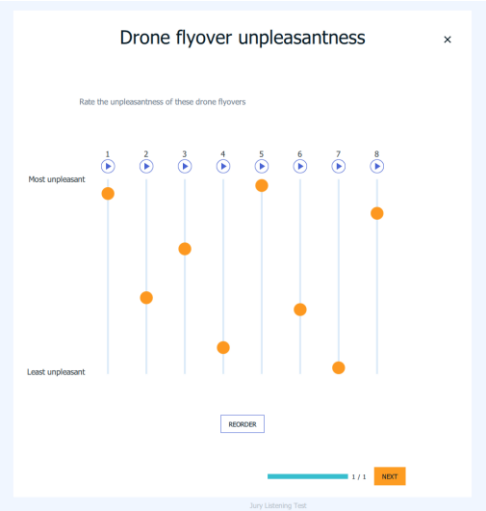

Figure 7. Example of listening test interface.

Once unpleasantness ratings are obtained, it is very useful to relate them to signal-based psychoacoustic indicators. The explanation is two-fold:

- It makes it possible to predict from a perceptual point of view if the noise of a given VTOL during a flyover is deemed acceptable or not.
- It provides a signal target to meet when creating new VTOL designs.

This method was successfully used in the case of commercial aircraft to identify relevant indicators for this type of noise source [22,23]. Before considering the possibility to define new indicators for the specific case of VTOL flyover, it is important to assess how these indicators can help objectify the unpleasantness ratings of VTOL flyovers.

Although various indicators can be found in the literature for aircraft unpleasantness, two perceptual aspects gather the most attention: Loudness and Tonality. Loudness is the perceptual equivalent to sound intensity; it takes into account how the sound is processed by human ears to produce a loudness sensation. Tonality, on the other hand, is a property that some sounds have where one or several strong tonal components stand out of the overall noise, to such a degree that they are distinctively audible. Unpleasantness is almost systematically found to increase with both loudness and tonality. This trend led to the creation of a specific indicator for aircraft flyovers that is currently used for certification: the Effective Perceived Noise Level (EPNL). This indicator is mostly based on a loudness indicator, to which correction factors are applied to account for isolated tonal components, and flyover duration. Many studies have proven that this indicator is highly suitable for predicting the unpleasantness associated with an aircraft flyover [22]. However, it was also shown that when sources include more complex tonal components, the tone correction factor included in the EPNL might be insufficient, and alternative tonality indicators help improve the predictions [23]. These findings should certainly be confronted with the results obtained for VTOL sources where several non-harmonic tonal components are present due to the multiple rotors with uneven rotational speed.

6. CONCLUSIONS

This paper reports on a comprehensive process that allows manufacturers to simulate the noise of a drone/eVTOL and, by considering human perception, reduce the noise annoyance. The main steps to simulate the noise of drones and eVTOLs from the source to the ground are detailed. In order to improve and validate this modelling several measurement campaigns are done for small and mid-size drones. Their analysis is still in progress, but it should provide valuable inputs to further generalize this process to be used for a large variety of VTOL vehicles as categorized in [1]. This will eventually allow manufacturers to assess the perceptual impact of their products' noises very early on, and thus help refine their designs at a limited cost.

7. REFERENCES

[1] S. Rizzi, D. Jr Huff, P. Bent, B. Henderson, K. Pascioni, D. Sargent, D. Josephson, M. Marsan, H. He and R. Snider. "Urban Air Mobility Noise: Current Practice, Gaps, and Recommendations". *Proc. of Internoise 2020*, Seoul, South Korea, 2020.

[2] Sparrow, V & Gjestland, Truls & Guski, Rainer & Richard, Isabelle & Basner, M & Hansell, A & Kluizenaar, Y & Clark, C & Janssen, S & Mestre, Vincent & Loubeau, A & Bristow, Abigail & Thanos, Sotirios & Vigeant, M & Cointin, R. (2019). *Aviation Noise Impacts White Paper*.

[3] European Union Aviation Safety Agency. (2020). Commission Regulation (EU) 2020/639 of 12 May

2020 on Unmanned Aircraft Systems and on Third-Country Operators of Unmanned Aircraft Systems. Official Journal of the European Union, L 143, 5-77.

[4] Federal Aviation Administration. (2016). Advisory Circular AC 36-1H: Noise Levels for U.S. Certificated and Foreign Aircraft.

[5] Federal Aviation Administration. (2020). Notice of Proposed Rulemaking: Remote Identification of Unmanned Aircraft Systems.

[6] A. Minard, S. Hourcade, C. Lambourg, and P. Boussard, "Sound synthesis and 3D sound rendering of aircraft flyovers with controllable parameters" *Proceedings of 22nd AIAA/CEAS Aeronautics Conference*, Lyon, France, June 2016.

[7] D. Caridi, "Industrial CFD Simulation of Aerodynamic Noise", PhD Thesis, University of Naples Federico II, Italy, 2008.

[8] Russell, Daniel & Titlow, Joseph & Bemmen, Ya-Juan. (1999). Acoustic monopoles, dipoles, and quadrupoles: An experiment revisited. American Journal of Physics. 67. 660-664. 10.1119/1.19349.

[9] Davydov, I. & Leontev, A. & Kozhevnikov, V. & Boldyrev, Y. (2018). On the selection of the method for solving the problem of external acoustics of an altitude propeller. Journal of Advanced Research in Dynamical and Control Systems.

[10] Chambon, Joannès & Minck, Olivier & Bouley, Simon. (2022). Dipolar-based equivalent sources method for 3D aeroacoustic source identification.

[11] Wangqiao, Chen & Jiang, Hanbo & He, Weishu. (2022). Dipole source-based virtual three-dimensional imaging for propeller noise. Aerospace Science and Technology. 124. 107562. 10.1016/j.ast.2022.107562.

[12] Kinsler, L. E., Frey, A. R., Coppens, A. B., & Sanders, J. V. (1999). Fundamentals of acoustics (4th ed.). John Wiley & Sons.

[13] ISO 9613-2:1996 Acoustique — Atténuation du son lors de sa propagation à l'air libre — Partie 2: Méthode générale de calcul

[14] Jónsson, Gunnar & Jacobsen, Finn. (2008). A Comparison of Two Engineering Models for Outdoor Sound Propagation: Harmonoise and Nord2000. Acta Acustica united with Acustica. 94. 10.3813/AAA.918031.

[15] Bianco, Michael & Gerstoft, Peter & Traer, James & Ozanich, Emma & Roch, Marie & Gannot, Sharon & Deledalle, Charles & Li, Weichang. (2019). Machine learning in acoustics: a review.

[16] Mishchenko, M. I., Travis, L. D., & Lacis, A. A. (2002). Scattering, absorption, and emission of light and sound by small particles. Cambridge University Press.

[17] Bian, Haoyu & Fattah, Ryu & Sun, Yuhao & Zhang, Xin. (2019). Noise prediction of drones in urban environments. 10.2514/6.2019-2685

[18] Madden, Michael. (2018). Verifying Implementation of the Dryden Turbulence Model and MIL-F-8785 Gust Gradient. 10.2514/6.2018-3580.

[19] Benzi, Roberto & Biferale, Luca. (2015). Homogeneous and Isotropic Turbulence: A Short Survey on Recent Developments. Journal of Statistical Physics. 161. 10.1007/s10955-015-1323-9.

[20] Allen, J. B., and Rabiner, L. R., "A Unified Approach to Short-Time Fourier Analysis and Synthesis," *Proceedings of IEEE*, Vol. 65, No. 11, 1977, pp. 1558-1564.

[21] A. Minard, B. Mellot, J.-F. Sciabica, "Aircraft noise unpleasantness: impact of different signal portions on overall assessment", *Proc. of Euronoise 2018*, Heraklion, Greece, 2018.

[22] I. Boullet, A. Minard, N. Pellegrin, P. Boussard, "Optimized tools and process for a better prediction of future aircraft noise perception", Proc. of Internoise 2023, Chiba, Japan, 2023.

[23] A. Minard, C. Lambourg, P. Boussard, "Signal-based indicators for predicting the effect of audible tones in the aircraft sound at takeoff". *Proc. of Internoise 2016*, Hamburg, Germany, 2016.